The thermodynamic basis for the binding of lipids to annexin a5

A THESIS

SUBMITTED TO THE FACULTY OF THE GRADUATE SCHOOL

OF THE UNIVERSITY OF MINNESOTA

BY

Kristofer James Knutson

IN PARTIAL FULFILLMENT OF THE REQUIREMENTS

FOR THE DEGREE OF

MASTER OF SCIENCE

Prof. Anne Hinderliter, Advisor

December 2009

ACKNOWLEDGEMENTS

I would first like to thank Dr. Anne Hinderliter for her patience and direction during my stay in her lab. Also, I would like to thank my wife for her understanding that science takes a great deal of time. I also thank her for the many delicious lab meals and cookies that made this research possible. I want to thank Dr. Steven Berry for his direction and helpfulness in guiding my research and for the use of several pieces of equipment that aided in annexin purification. Also, without the help of students: Emily Frey, Jake Gauer , Andy Houghton, Jesse Murphy , Zach Nelson, and Ryan Sisk this work would not have been possible. In addition, I would also like to thank my friends; Greg Rhode, Jeff Carlson, Kelly Brevik, and Jason Dorweiler for keeping life both inside school and out interesting. I would like to thank my family for their emotional support over the last few years. Without the help of the UMD secretaries and Neil Weberg, this project would have been much more difficult. Also, I would like to thank God for leading me down this interesting path.

ABSTRACT

Protein-membrane interactions are a vital mechanism of propagating signals both across the membrane and between cells. To control the magnitude and specificity of this type of cell signaling at the membrane, clustering of similar lipids and proteins has been observed in the cell via the formation of lipid microdomains. To address the thermodynamic basis of lipid induced signal propagation, we investigated how lipid microdomains form in response to annexin a5 binding to model membranes using Isothermal Titration Calorimetry (ITC). Annexins are known to bind to negatively charged (e.g., phosphatidylserine [PS]) membranes in a Ca^{2+}-dependent manner. Based on Differential Scanning Calorimetry (DSC) results, we suggest that annexin functions to order lipid acyl chains upon binding and that the ordering of phospholipids can lead to the formation of microdomains. Using ITC, we have analyzed the membrane binding affinity of annexin for both gel and fluid state mixtures. Binding analysis of these isotherms shows that annexin binds fluid state mixtures with a significantly lower K_d than gel state (acyl chain ordered) lipids, which would be consistent with the hypothesis that binding of annexin a5 orders the acyl chains of the phospholipids. In addition, because the binding is entropically dominated but exhibits greater affinity for fluid compared to gel state lipids, we suggest that annexin binding is driven by the release of water molecules and ions as fluid lipids have more waters of hydration. Interestingly, the enthalpy associated with the binding process for both gel and fluid state lipid mixtures is small, indicative of a weak enthalpic association and suggestive of

entropically mediated binding. We also present the binding of Eu^{3+} by a lanthanide binding complex (Tetra(N-(tert-butyl)-acetamide)-1,13-diamino-3,6,9-trioxadecane).

TABLE OF CONTENTS

ABBREVIATIONS

Anx5	Annexin 5 (no specific reference)
anxa5	Rat annexin a5 (recombinant)
BME	Beta-Mercaptoethanol
$CaCl_2$	Calcium Chloride
DMPC	1,2-dimyristoyl-*sn*-glycero-3-phosphocholine (14:0 PC)
DMPS	1,2-dimyristoyl-*sn*-glycero-3-phospho-L-serine (14:0 PS)
DSC	Differential Scanning Calorimetry
FRET	Fluorescence Resonance Energy Transfer
HEPES	(4-(2-hydroxyethyl)-1-piperazineethanesulfonic acid)
IPTG	Isopropyl β-D-1-thiogalactopyranoside
ITC	Isothermal Titration Calorimetry
LUV	Large Unilamellar Vesicle
$MgCl_2$	Magnesium Chloride
mM	Millimolar
MOPS	3-(N-morpholino)propanesulfonic acid
PMSF	Phenyl methyl sulfonyl fluoride
POPC	1-palmitoyl-2-oleoyl-*sn*-glycero-3-phosphocholine (16:0,18:1PC)
POPS	1-palmitoyl-2-oleoyl-*sn*-glycero-3-phospho-L-serine (16:0,18:1 PS)
SDS-PAGE	Sodium Dodecyl Sulfate Polyacrylamide Gel Electrophoresis
μM	Micromolar

LIST OF FIGURES

LIST OF TABLES

Scope of this Thesis

This thesis presents the characterization of metal binding using thermodynamics as a diagnostic technique. The first chapter is an introduction to lipid membrane interactions. The second chapter discusses the purification of anxa5, as well as the synthesis of a mutant annexin to be used for FRET analysis. The third chapter presents a characterization of lipid binding by anxa5 via the use of DSC. The fourth chapter discusses the use of ITC to determine the thermodynamic impetus of annexin-membrane binding. The fifth chapter presents the binding of Eu^{3+} by a lanthanide binding complex.

CHAPTER 1: ANNEXIN-LIPID INTERACTIONS

1.0 INTRODUCTION AND BACKGROUND

The interaction between proteins and the membrane is essential for both cellular communication and homeostasis. Defining the structure and function of biological membranes has been a part of biological research since the early 1800s. These interactions have been investigated by several methods ranging from biophysics to molecular biology, and have been under intense investigation recently as the role of "lipid rafts" has gained considerable research interest. The membrane is the interface between the cell's external and internal environment, playing an integral role in the life and activity of a cell. Culminating on the work of their predecessors, Singer and Nicolson proposed the fluid mosaic model (*1*). The model describes the membrane as having a phospholipid bilayer with embedded proteins. The mosaic is represented by a scattering of proteins in and on the membrane surface with fluid lipid components that are free to diffuse laterally. A variety of lipids, primarily phospholipids, glycolipids, and sphingolipids, together with a number of sterols, make up the membrane's bilayer. The concentrations present, as well as how these components interact, can have important consequences for the structure of the membrane. Utilizing these concepts, several groups pioneered the expansion of the fluid mosaic model to include different phases of the lipid membrane including liquid ordered, liquid disordered, and gel state lipids (*2-3*). The findings of these groups suggested that small, cooperative interactions between lipids can have large impacts on domain size as lipids approach a phase transition boundary which can influence the formation of signal transduction complexes (*4*). In the physiological state, lipids are usually comprised of acyl chains with unsaturations present and exist in a

liquid-disordered state. In the liquid disordered state, a cis conformation predominates and the lipid tails assume a "kinked" confirmation allowing for more flexible rotation. When lipids assume the kinked conformation, the membrane has greater fluidity since the lipid tails do not have Van der Waals interactions with other lipid tails as occurs in the gel state (*5*). In physiological systems, gel state lipids do not often exist (other than in the lung) (*6*). Gel state lipids exist in a conformation in which side chains are highly saturated and fully extended. This allows lipid headgroups and their respective side chains to line up very closely together, forming a highly compacted rigid structure in which free rotation of the lipid tails becomes sterically hindered. Membrane fluidity must be carefully balanced, given that a too rigid or leaky of a structure would effectively destroy the cell's ability to maintain an environment capable of carrying out cellular activities.

The shape of cholesterol allows it to insert itself between membrane lipids, filling in gaps and lending to a more rigid structure. This combination of lipids and cholesterol can create a liquid-ordered state that can be present as a heterologous distribution of lipids throughout a liquid disordered membrane (*7-8*). These "lipid rafts" (here we will call them microdomains) were discovered as an insoluble fraction during treatment with the nonionic detergent Triton X-100 (*9-10*). In addition, certain proteins were repeatedly found in the insoluble fraction, leading to the hypothesis that these proteins, some of which are involved in signal transduction processes, interact selectively with lipid rafts (*11*). The phase changes that occur when forming lipid rafts appear to play a key role in determining membrane protein distribution and organization (*12*). A protein can influence the heterogeneity of the membrane surface and the formation of the

microdomains if the protein has selectivity of one type of lipid over another. The signaling cascade induced by the formation of lipid microdomains has stimulated research into how both similar and dissimilar lipid types interact, and how protein interactions with these heterogeneities can influence cellular communication. Therefore, the membrane exists not as a static protective surface, but as a dynamic structure whose components display non-random behavior that is controlled by a multitude of factors.

By understanding the mechanism of action of membrane binding proteins, specifically the thermodynamics of membrane binding, the foundation for many cellular processes can be better understood. Following a membrane-protein interaction, the organization of differential membrane lipid species can propagate signals both across the lipid membrane and on the interior of the cell, often playing a vital role in the outcome of cellular fate and exocytotic events. The breakdown of signaling arising from lipid organization has been implicated in diseases such as Diabetes, Alzheimer's, and Atherosclerosis (*13*). Therefore, critical understanding of how a model protein, anxa5, influences membrane organization is important to the therapeutic treatment of numerous diseases and the understanding of cellular signaling.

The annexins are a class of peripheral membrane bound proteins that have been shown to associate with and influence the formation of microdomains (*14*). However, the specific mechanism by which they achieve this remains unclear. As a group, the annexins are classified based on a highly conserved core domain and their ability to bind both Ca^{2+} and acidic phospholipids (such as 16:0,18:1 Phosphatidylserine (POPS)). Interest in the annexins stem from their ubiquitous nature in eukaryotes (with the exception of yeast and protists), representing up to 2% of intracellular protein (*15*).

Despite their overwhelming occurrence, finding any specific function of the annexins has been difficult. Current studies have suggested that annexins can have numerous functions, including acting as membrane-membrane linkers, functioning as cytosolic linkers, and acting in Ca^{2+} regulated exocytotic events. Due to their respective location on the plasma membrane they have also been thought to regulate endocytosis and corresponding stabilization of specific domains on both organelles and in the plasma membrane (*16*). Several disease states that correspond with the functions of annexins vary from pathogenic infections to anti-phospholipid syndrome (*17*).

The highly diverse functions attributed to the annexins likely correspond to the structure of their N-terminus, which varies with each member of the annexin family. The conserved core domain responsible for both Ca^{2+} and lipid binding is composed of four "annexin repeats," comprised of five alpha helices, each approximately 70 residues in length (*16*). The convex binding cleft in annexins for Ca^{2+} and lipid binding on the interior portion of the plasma membrane is on the "bottom" of the protein while the "top" is responsible for interactions with other proteins via the N-terminal domain (Figure 1). The structural rearrangements caused by the N-terminal domain integrating with the core of annexin proteins causes a shift in the protein to a more rigid structure (*18*), which would be consistent with this hypothesis that the N-terminal domain can modulate stability and Ca^{2+} binding affinity (*18*). It is possible that the variability in both length and sequence of the N-terminal domain could change the binding affinity for Ca^{2+} or membrane for each class. This could provide explanation for the large variety of homologous annexins found in eukaryotes as the length of the N-terminal domain could

alter the affinity for ligand, or provide different sites for Post-translational modifications as evidenced in (*19*).

Ca^{2+} binding in the annexin group is a function of the concentration of both membrane and protein (*20*). Several factors influence the affinity of annexin for Ca^{2+} and are as follows: length of N-terminal tail, type of bound/unbound lipid, and number of helical repeats found in the annexin structure. Due to variability found in the N-terminal region of this protein, it has been suggested that certain annexins, such as annexin a4 and a5, bind Ca^{2+} by an allosteric transition model (*21*). In the allosteric model for annexin binding to the lipid membrane, binding to the phospholipid membrane switches the Ca^{2+} binding activity from a low affinity to a high affinity state. An extended N-terminal tail, found in annexin 2 for example, may also function in the bridging of membrane in the absence of previously bound Ca^{2+} (*22*).

The characteristic Ca^{2+} binding sites of the annexins are found with the "endonexin fold" in each of the four helical repeats of the annexins. In these respective folds, Ca^{2+} is bound to the consensus sequence, Glycine - Variable Amino Acid – Glycine - Threonine (G-X-G-T). In contrast to other Ca^{2+} binding domains such as the calmodulin (EF hand) domain, the Ca^{2+} binding domain in the annexins family has a variable amount of Ca^{2+} ions bound depending on the crystallographic study. These structures can have up to a maximum of 12 Ca^{2+} ions bound (*23*). Of the annexin family, Anx5 has been shown to have the highest Ca^{2+} concentration requirement for binding to phospholipids for which several mechanisms have been hypothesized. Recently, the allosteric model of Monod, Wyman, and Changeux (*24*) has been proposed for anxa5 binding (*21*). Similar to the T and R states for hemoglobin, anxa5 displays two affinities

for Ca^{2+} depending on being lipid bound or not. When lipid is not present, anxa5 displays a hyperbolic curve for the binding of Ca^{2+}, which is characteristic of independent binding. Upon binding lipid, the affinity of anxa5 is increased toward Ca^{2+} resulting in weakly cooperative binding.

Another important aspect of the binding of the annexins to membrane is the formation of annexin trimers on the membrane surface during a membrane binding event. Annexins have been shown to trimerize using cryo-electron microscopy and form two types of 2D crystals with either p6 or p3 symmetry (*25*). Membranes bound by Anx5 exhibit drastic changes in their properties, becoming significantly more rigid as the crystallization domains (trimers) increase in size (*26-28*). Also, clustering of acidic lipids has been demonstrated by (*29*), which would be consistent with the hypothesis that annexin functions to order the membrane by creating patches of acidic phospholipid. The trimerization process of Anx5 on the membrane surface is believed to play a functional role in processes associated such as emergency repair of membranes. (*30*)

CHAPTER 2: SYNTHESIS OF ANNEXIN A5

2.0 INTRODUCTION

2.1 SYNTHESIS OF ANNEXIN

Purification of wild-type *Rattus norvegicus* anxa5 was based on Ca^{2+}-dependent binding to membrane previously developed in (*31*) with slight modifications. The plasmid for recombinant anxa5 production was generously provided by Hitoshi Sohma in the Novagen pET3d plasmid. (*21*) The pET3d plasmid was transformed into the Bl-21 (DE-3) (Stratagene) cell line and periodically checked to ensure that the sequence of the construct remained intact. DNA sequencing was conducted by the UMN core sequencing

facility. To begin protein production, small 5 ml overnight cultures were started from inoculation with a single colony. The plasmid contained ampicillin resistance and a concentration of 100 μg/ml was used for all media. Large 1 liter cultures were inoculated from the small 5 ml cultures and allowed to grow to induction range optical densities. Expression of anxa5 was induced by addition of 1mM IPTG at optical densities ranging from 0.8-1.6 in transformed Bl-21 cells containing the plasmid for anxa5. After a five-hour induction period, cells were harvested by centrifugation, and lysed via sonication in 20mM MOPS, 100mM KCl, 1mM PMSF, and 10mM $CaCl_2$ pH 7.50. Utilizing the Ca^{2+}-dependent binding properties of anxa5 as a purification technique, the anxa5 binds to the acidic phospholipids in bacterial membranes in the presence of Ca^{2+} and can be separated from the rest of the protein milieu. Because bacteria do not use Ca^{2+} in signaling, they do not have Ca^{2+} enhanced membrane binding proteins. Following sonication, cellular debris and anxa5 were pelleted by centrifugation at 16,000rpm for 30 minutes. The pellet containing anxa5 was then resuspended in 20mM MOPS, 100mM KCl, 20mM EDTA, 1mM BME pH 7.50 and allowed to mix overnight facilitating the release of anxa5. The mixture was then centrifuged to remove cellular debris and sterile filtered using a 0.45μm filter followed by dialysis against 20mM HEPES, 5mM $MgCl_2$, pH 8.00. Following dialysis, the supernatant was incubated with Benzonuclease (Novagen 90% purity) at a concentration of 10units/ml for 6-8hrs at 4°C to remove contaminating nucleic acids. Further purification was performed using pre-equilibrated Q-Sepharose Fast Flow media (anion exchange column). Purified protein was dialyzed against 20mM HEPES, 1mM BME, pH 8.00, and eluted using a linear gradient of NaCl containing 20mM HEPES and 1mM BME. Pure anxa5 eluted at 200mM NaCl and fractions containing pure

recombinant anxa5 were then pooled and filtered using a 0.20µm filter. Following the pooling of the samples, SDS-PAGE was used to determine purity, and occasionally gel filtration was used to remove any contaminating bands. Anxa5 was dialyzed with extensive dialysis against 20mm MOPS, 100 KCL pH 7.50. Recombinant anxa5 protein was then passed through Chelex-100 resin to remove contaminating Ca^{2+} and concentrated to ~30mg/ml through the use of Amicon concentrator units with a 30kDa cutoff. Final purity of anxa5 was >95% as judged by SDS-PAGE densitometry and concentration was determined either using the Bradford method or the use of a Nanodrop with an extinction coefficient of $21{,}050M^{-1}$. This purification technique was found to produce more than 15mgs/liter of pure, recombinant anxa5. This is in contrast with the inclusion body protocol (*32*) which was found to produce a disappointingly low yield of 1-2mg/liter. More significantly, however, was the reduction of contaminating protein bands that were found in inclusion body purification methods. It was found that at lower yields, the inclusion body purification method was found to produce >95% pure anxa5. When protein purification yield was greater than 5mg/ml, however, the appearance of contaminating bands intensified indicating that a protein-protein (anxa5-with unknown) interaction was likely the cause of the contamination (Figure 2).

2.1.1 QUALITY CONTROL OF ANNEXIN SYNTHESIS

In our current lipid affinity purification protocol, removal of contaminating bands was achieved by the addition of 1mM BME during the anion exchange process (Figure 2). As an additional quality control, DSC was performed to determine the validity of the purification method and the foldedness of the protein (Figure 3). DSC is a valid method for the determination of the denaturation temperature (T_m) and ΔH for

proteins (*33*). It is difficult to compare the results of our work with the previous denaturation of annexin due to different buffer usage and different protein concentrations (*32*). The work of Rosengarth et al, (*32*) obtained an enthalpy 163.0 kcal/mol and a T_m of 52.5°C versus our experimentally obtained enthalpy of 140.1 kcal/mol and T_m of 50.4°C (Figure 3). It must be considered that the buffer used in the work of Rosengarth was in 50mM Tris Buffer, 100mM KCl at pH 8.0 and that they used a low protein concentration (12μM). It has been well documented that Tris has a large heat of ionization (*34*) ~12kcal/mol and has a large pH variation over the heating process, making it an unsuitable buffer for DSC analysis. Also, it has been shown that annexin is more stable at higher pH's (*32*). The difference in pH, concentration, and buffers are the likely reasons for the disagreement between the data. Similar to other groups, we were unable to generate reversibility (*35*).

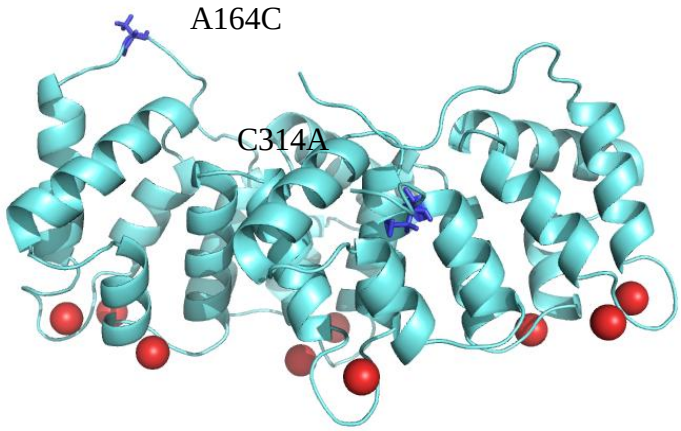

Figure 1 Annexin a5 Mutant Design. A cysteine was introduced in position A164C, the endogenous cysteine was changed to an alanine, C314A. Both mutations highlighted in blue and stick form. Spheres represent Ca2+ ions.

2.1.2 SYNTHESIS OF ANNEXIN MUTANT C314A, A164C

In addition to the synthesis of anxa5, we sought to determine the influence of protein-protein interactions (specifically trimerization) on anxa5 binding to membrane. To address this experimentally, a mutant (A164C, C314A) was synthesized using site directed mutagenesis. Despite correct sequencing following mutagenesis, multiple attempts to produce the protein using inclusion body purification and the membrane lysate purification described here were limited by extremely poor yield of the mutant protein. It appears as though the insertion of a cysteine at site 164 has introduced the formation of multiple aggregates which could be a result of misfolded, aggregated protein that was irreversible even in the presence of BME and dithiothreitol (DTT).

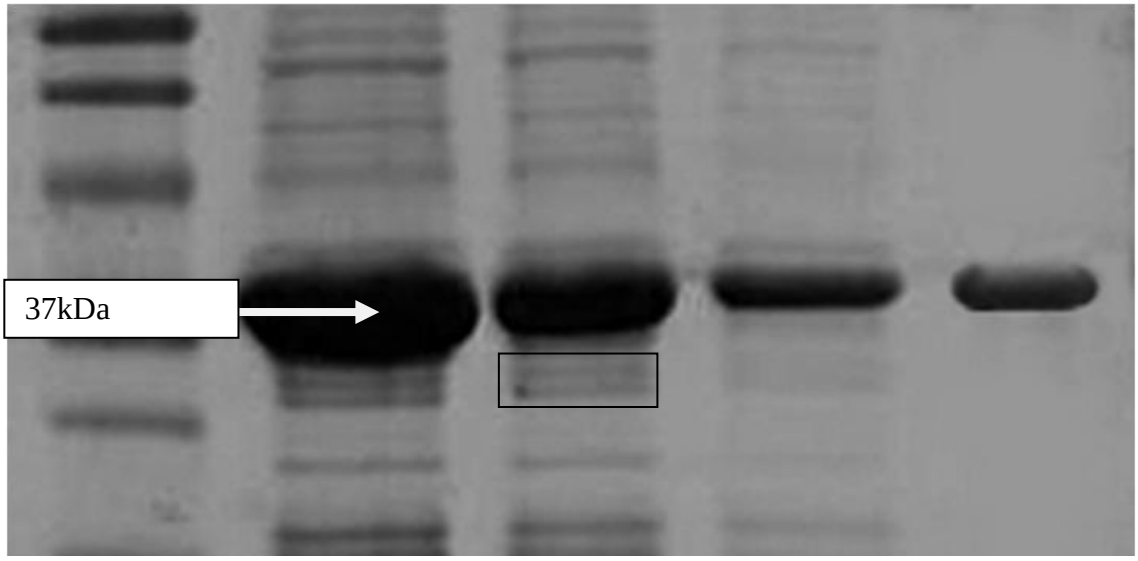

Figure 2 Scheme of anxa5 purification. From left to right (Lysis, Membrane Bound, Benzonuclease Treatment, Final Annexin.) Boxed bands indicate contaminating bands present in Inclusion body purification method.

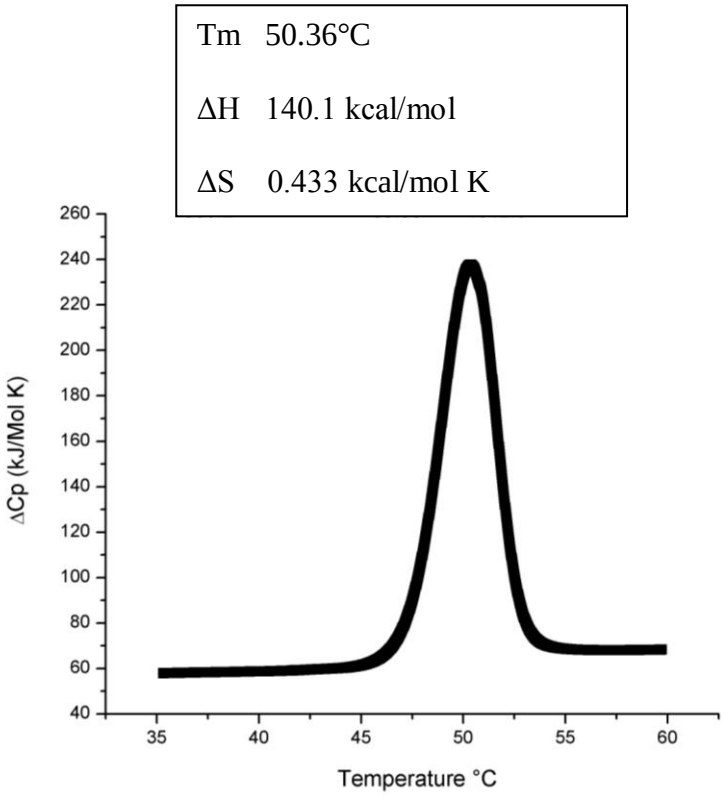

Figure 3 DSC Thermogram of 84µM anxa5 in the absence of ligand.

CHAPTER 3: DIFFERENTIAL SCANNING CALORIMETRY OF ANNEXIN A5 WITH GEL STATE LIPIDS

3.0 DSC THEORY

To thermally denature a protein, sufficient heat must be added to the system to overcome interactions that maintain the protein's higher order structure. This additional requirement of heat can be thought of as a phase transition. Phase transitions can also exist in lipids, such as the gel state to fluid state transition. In either case, such phase transitions are the result of many relatively small interactions, and are often much smaller than the heat absorbed by water. This fact makes it difficult to determine the magnitude of these interactions directly with conventional calorimetry. Differential scanning calorimetry circumvents this problem by measuring the heat necessary to raise the temperature of a buffered sample against a buffer alone. By measuring a difference, and thereby removing the relatively large baseline heat capacity contribution of water, we are able to characterize these interactions.

3.1 DIFFERENTIAL SCANNING CALORIMETRY METHODS

Differential scanning calorimetry scans were conducted on a TA Instruments Nano DSC calorimeter. 16.5mM lipid sample comprised of 60%:40% 14:0PC (DMPC): 14:0 PS (DMPS) in a buffer of 20mM MOPS, 100mM KCl at pH 7.50 was scanned repeatedly back and forth from 0°C - 75°C with a scan rate of 0.2°C per minute until equilibrium was reached and the observed endotherms overlapped. Upon reaching

equilibration, the lipid mixture was diluted and Ca^{2+} and buffer were added. This mixture was scanned in the same fashion until overlapping transitions were observed. Finally, recombinant anxa5 (produced via the method of (*32*)) was added, and the mixture was scanned once from 0°C - 75°C. This experiment was repeated using two concentrations of Ca^{2+} (0.75mM and 1.87mM) corresponding to 95% and 99% saturation of anxa5 by Ca^{2+}, respectively. These saturation levels were determined using binding constants for Tb^{3+} in POPC:POPS mixtures (*21*). Lipid concentrations were confirmed post-DSC by phosphate assay (*36*).

3.2 DIFFERENTIAL SCANNING CALORIMETRY RESULTS

The lipid mixture of 14:0PC (DMPC) and 14:0 PS (DMPS) Large Unilamellar Vesicles (LUVs) has a characteristic endotherm with increasing temperature due to the transition of the lipid acyl chains from an ordered (gel) to disordered (fluid) state (Figure 4). The resultant endotherm had a transition peak of 26.4°C and an associated enthalpy of 7.45 kcal/mol. Upon addition of 1.872 mM Ca^{2+}, the T_m of the lipid mixture decreased from 26.8°C to 25.2°C. This reduction in T_m is accompanied by a differentiation of the endotherm into PS and PC enriched regions of the endotherm. Pure DMPS melts at 35°C and DMPC at 23°C (*37*). The addition of Ca^{2+} also induced a significant reduction in the entropy and enthalpy, from 0.0248 kcal/molK to 0.0156 kcal/molK, and 7.45 kcal/mol to 4.64 kcal/mol, respectively. This is presumably due to the cation-induced ordering of the lipid acyl chains (*38*). This concentration of Ca^{2+} corresponded to 99% saturation of anxa5 by Ca^{2+}. Upon addition of anxa5, there was a small upward shift in T_m from 25.2°C to 26.1°C as well as a small, but statistically significant reduction in entropy from 0.0156 kcal/molK to 0.0146 kcal/molK and in enthalpy from 4.64 kcal/mol to 4.38

kcal/mol (Figure 4 & Table 2). To more sensitively isolate the impact of protein binding upon lipid acyl chain ordering from the influence of Ca^{2+}, the experiment was repeated with a lower level of Ca^{2+} saturation (from 1.872 mM Ca^{2+} to 0.75 mM Ca^{2+}). In the presence of 0.75 mM Ca^{2+}, the T_m of the lipid mixture decreased from 26.4°C to 25.8°C. The addition of this smaller concentration of Ca^{2+}, induced a lesser reduction of the entropy and enthalpy from 0.0251 kcal/molK to 0.0214 kcal/molK and from 7.50 kcal/mol to 6.39 kcal/mol, compared to the 99% saturation data. The addition of anxa5 increased the T_m to 29.7°C and a decrease in entropy and enthalpy to 0.0187 kcal/molK and to 5.66 kcal/mol, respectively.

The T_m of the Ca^{2+}/lipid mixture shifts upward in the presence of anxa5, consistent with a protein-induced ordering of the lipid acyl chains. This observation has led to the working hypothesis that such ordering is a means to alter the lateral distribution of lipids. Ordered lipids will interact differently with other lipids and themselves than with bulk fluid state lipids. This change in the excess free energy by ordering of the lipids upon anxa5 binding is a means to propagate the free energy change in the membrane, thereby altering lipid distribution. A ramification of lipid ordering and water mediated selectivity is that the resultant smaller headgroup of the phospholipids will lead to lateral compression and greater ordering of the acyl chains of the lipids.

Table 1 DSC results at 99% saturation for anxa5 (Corresponds to Figure 4 Panel A)

99% Experiment	**ΔH (kcal/mol)**	**T_m (C)**	**ΔS (kcal/molK)**
13.1mM DMPC:DMPS 60:40	7.45	26.8	0.0248
8.7mM DMPC:DMPS 60:40 1.87mM Ca^{2+}	4.64	25.2	0.0156
4.4mM DMPC:DMPS 60:40 1.87mM Ca^{2+} 73μM annexin a5	4.38	26.1	0.0146

Table 2: DSC results at 95% saturation for anxa5 (Corresponds to Figure 4 Panel B)

95% Experiment	**ΔH (kcal/mol)**	**T_m (C)**	**ΔS (kcal/molK)**
16.5mM DMPC:DMPS 60:40	7.50	26.4	0.0251
9.4mM DMPC:DMPS 60:40 0.75mM Ca^{2+}	6.39	25.8	0.0214
4.9mM DMPC:DMPS 60:40 0.75mM Ca^{2+} 75μM annexin a5	5.66	29.7	0.0187

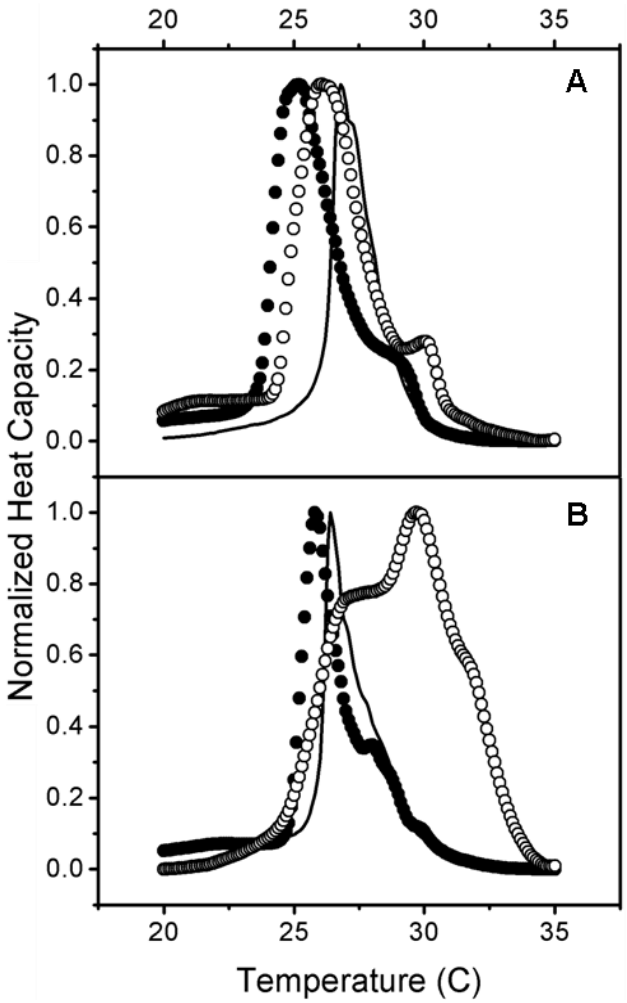

Figure 4 DSC Thermogram of anxa5 with DMPC:DMPS LUVs

All lipid samples consist of a 60:40 mixture of DMPC:DMPS (14:0,14:0PC:14:0,14:0PS).

Panel A – *Solid Line:* 13.1mM total lipid. *Closed Circles:* 8.7mM total lipid the presence of 1.87mM Ca^{2+}. *Open Circles:* 4.4mM total lipid in the presence 1.87mM Ca^{2+} and 73µM anxa5. At this concentration of Ca^{2+} the anxa5 approximately 99% saturated with Ca^{2+}

Panel B - *Solid Line:* 16.5mM total lipid. *Closed Circles:* 9.4mM total lipid in the presence of 0.75mM Ca^{2+}. *Open Circles:* 4.9mM total lipid in the presence of 0.75mM Ca^{2+} and 75µM anxa5. At this concentration of Ca^{2+} the anxa5 approximately 95% saturated with Ca^{2+}

CHAPTER 4: ISOTHERMAL TITRATION CALORIMETRY OF ANNEXIN A5

4.0 ITC THEORY

When trying to understand a biological process, it is often important to not just know that an event is happening, but also the strength and specificity of the reaction. ITC is a technique that allows the determination of the thermodynamic parameters, binding constant (K_a) and binding stoichiometry in a single experiment. When substances bind, heat is either generated (exothermic) or absorbed (endothermic). ITC is a thermodynamic technique that directly measures the heat released or absorbed during a biomolecular binding event and uses the relationship $\Delta G = -RT \ln K_a$ to define the binding constant and thermodynamic parameters of a reaction. To accomplish this, the instrument utilizes two gold-plated cells (for maximal thermal conductivity) which are thermostated at the same temperature. During the course of the experiment, the instrument measures the energy it takes to keep the sample cell at the same temperature when a ligand is injected. This power difference is then converted into heat. Following conversion of the signal into heat, the total heat evolved from injection is then integrated and the total heat evolved per moles of injection can be calculated. As some heat effects evolve simply from injecting the ligand into buffer, a correction must be applied to the data. This is accomplished by injecting just ligand into protein dialysate in the absence of buffer. The heats evolved by this reaction are then subtracted from the experimental data and the heats can then be analyzed. In comparison to the use of fluorescence to determine the binding constant of these reactions, the use of ITC to characterize protein-lipid interactions requires significantly more material (mM) when compared to quantities required for fluorescence (nM). Another concern in the analysis of the ITC isotherms is

that the signal is the total heat given off or taken up and the source of this signal may not be as readily apparent as it is with other techniques. Buffer and pH mismatch between syringe and cell can be a significant source of heat that can completely overwhelm the heat of binding. (*39*). Therefore, typical ITC experiments require that protein used for experimentation be exhaustively dialyzed and that the ligand is prepared from the dialysate of the protein mixture (In this case lipid and Ca^{2+}).

4.1 ISOTHERMAL TITRATION CALORIMETRY METHODS

Isothermal titration calorimetry experiments to determine the thermodynamic parameters of binding of various lipids to anxa5 protein were performed on a TA Instruments© (New Castle, Delaware) Nano ITC at 15°C. Both the Ca^{2+} and lipid titrant were hydrated in protein dialysate consisting of 20 mM MOPS (99% Fluka Biochemika) and 100 mM KCl (Fluka Ultra) pH 7.5 that was passed through equilibrated Bio-Rad 100 chelex resin to remove cation impurities and filtered using a 0.2μm sterile filter. As protein and ligand concentrations are critical for the determination of binding stoichiometry in ITC experiments, the cell protein concentration was directly measured using the calculated extinction coefficient of 21,050 M^{-1} (*40*) at 280nm prior to the experiment. The syringe (titrant) lipid concentration was corrected for dilution following the experiment via phosphate assay (*36*). The Ca^{2+} stock used in ITC experiments was synthesized using Fluka Molecular Biology Ultra grade $CaCl_2$ and the concentration of Ca^{2+} was verified through the use of the BAPTA method (*41*) as well as a Ca^{2+} selective electrode (ThermoFisher). The pH of both the protein sample and titrant buffer was matched to pH 7.50, ensuring that no heat from the titration was a result of pH mismatch between the cell and syringe solutions. Prior to titrations, the cell was rinsed with 10

flushes of dialysate buffer to remove any contaminating water present in the cell prior to the experiment. The sample cell was filled with 1.300 mL of thoroughly degassed solution consisting of 0.029mM anxa5 and 0.5mM Ca^{2+} for fluid state experiments (POPC:POPS), or 0.100 mM anxa5 protein and 1.0mM Ca^{2+} for gel state (DMPC:DMPS) experiments. The syringe was loaded with 250 µl of 30mM total lipid and either 0.5mM Ca^{2+} for POPC:POPS experiments or 1.00mM Ca^{2+} for DMPC:DMPS experiments. The use of the same Ca^{2+} concentration in both the cell and the syringe allow just the heat of membrane binding to be investigated (Figure 8). The Ca^{2+} concentrations used represent 91% saturation for the gel state experiment and 95% for the fluid state experiment. The use of these Ca^{2+} concentrations minimizes the interference of the heat produced by the anxa5-Ca^{2+} binding event during the membrane titration. The reference cell was filled with degassed Milli-Q water and replaced every 1-2 weeks. The stir speed was 250 rpm and the interval between injections was 300 seconds. Lipid titrant was added in a 1 µl injection to displace air from the syringe followed by 27 x 9 µl injections for the POPS:POPC experiment and 19 x 13 µl injections for the DMPC:DMPS experiment. The raw heats were integrated and the heat of dilution subtracted. The heat of dilution was conducted by injecting the lipid and Ca^{2+} into buffer containing the same concentration of Ca^{2+} without protein. In between experiments, the sample cell was cleaned with a 15% Contrad-70©:15% methanol mixture, followed by a methanol rinse to remove any contaminating lipids. Following solvent cleaning, 5 liters of Milli-Q water was used to rinse the sample cell. A buffer-buffer titration was also conducted to ensure that non-specific heats in the buffer were not present. The subtracted heats were then fit using the independent binding model (single site of identical affinity) from TA

Instruments Bindworks© software and verified independently using the Wiseman isotherm (*42*) and the solver feature in Microsoft© Excel.

4.2 FITTING EQUATION

$$\frac{dQ}{d[X]_t} = \frac{\Delta H^{\circ} V_{\circ}}{2}\ 1 + \left[\frac{1 - \frac{[X]_t}{[M]_t} - \frac{n}{K_a [M]_t}}{\sqrt{\left(1 + \frac{[X]_t}{[M]_t} + \frac{n}{K_a [M]_t}\right)^2 - \frac{4[X]_t}{[M]_t}}}\right]$$ Wiseman Isotherm

Where :

n= Number of Binding sites of Equal Affinity *(FITTING PARAMETER)*

$[X]_t$ = Total Ligand Concentration

$[M]_t$ = Total Macromolecule (Protein) Concentration

K_a = Binding Constant *(FITTING PARAMETER)*

ΔH°= Enthalpy *(FITTING PARAMETER)*

$V_{\circ}$= Effective Volume of Calorimetric Cell (The effective volume is defined as the only the volume that heat can be measured from. For example, when the calorimeter cell overflows during the course of the titration the heat measured only includes the total active volume of the cell which is 0.950 mLs.)

dQ= Stepwise Heat Change during each point in the titration

$d[X]_t$= Stepwise Ligand Change during each point in the titration

4.3 ITC RESULTS

ITC results suggest that anxa5 preferentially binds PS-containing fluid state mixtures over gel state lipids with a K_d ($1/K_a$) of 13 μM^{-1} vs. 1700 μM^{-1}. There is some discrepancy between the binding stoichiometry between fluid and gel state titration which is likely due to the low 'c' (c = n* Ka) value for the gel state titrations. The Ca^{2+} binding stoichiometry of 6 Ca^{2+}ions per annexin molecule is within the range of reported values for binding stoichiometry (*21*) for Ca^{2+} and displays a much higher enthalpic contribution upon Ca^{2+} ligation in the binding pockets of Anx5 in comparison to lipid binding ΔH of-1.9 kcal/mol, respectively. This enthalpic contribution is likely due to the electrostatic nature of binding between anxa5 and divalent cations. Similar to other metal-binding proteins, anxa5 utilizes negatively charged amino acids to form favorable electrostatic interactions with Ca^{2+} ions.

Anxa5 displays an entropically dominated binding signature for membrane in both the fluid and gel state in which water and ions are released from the membrane surface upon binding. The lyotrophic mechanism is an event which dehydrates the membrane and induces order in the lipid mixture. For the fluid state titrations, we report an enthalpy of -0.274 ± 0.001 kcal/mol and entropy of 6.2 ± 0.2 kcal/mol. For titrations in which gel phase lipids are injected into anxa5 we report an enthalpy of 0.117 ± 0.003 kcal /mol and entropy of 3.8 ± 0.3 kcal/mol, respectively.

4.4 THERMODYAMIC CYCLE FOR ANX5 BINDING

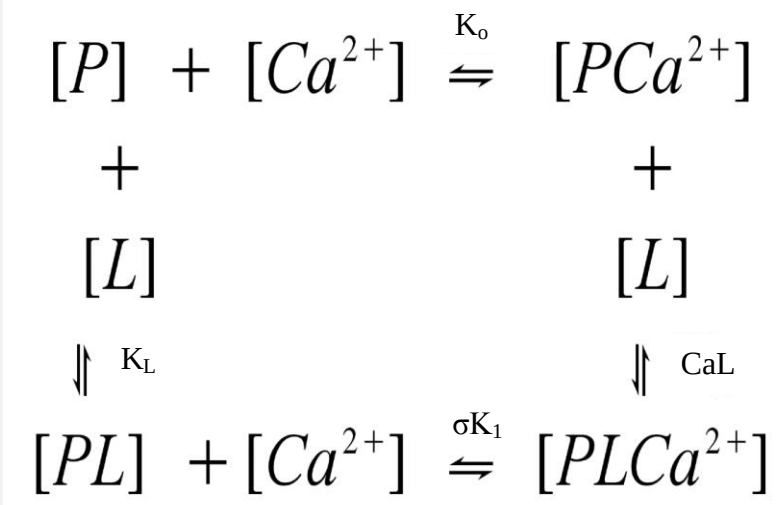

Figure 5 Thermodyamic Cylcle for Anx 5 with Ca^{2+} and Lipid binding
P=Anxa5, L=Lipid, Ca^{2+}= Calcium Ion

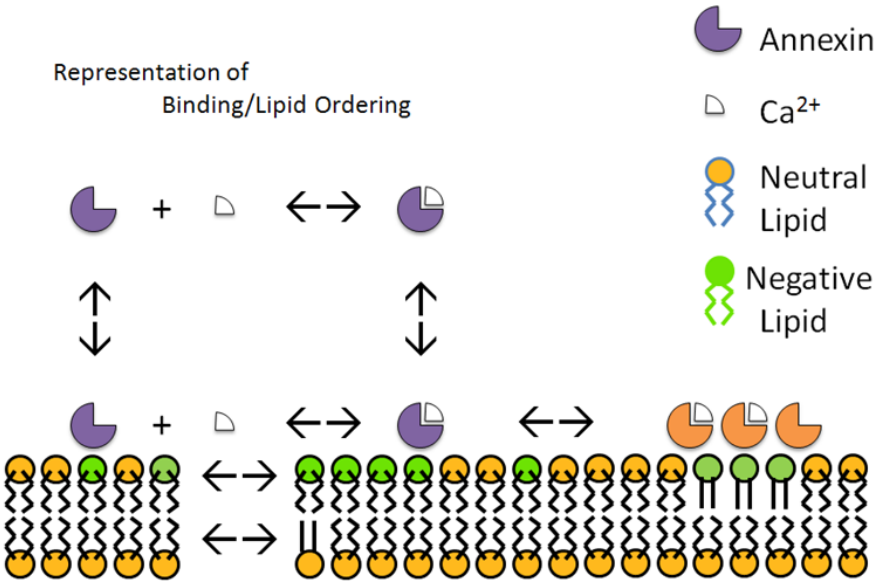

Figure 6 Representation of lipid ordering upon annexin binding

4.5 ITC DISCUSSION

ITC results suggest that anxa5 binds both fluid and gel state lipid mixtures in an independent manner (single binding site of identical affinity) with entropy dominating the binding (Table 3). Although it has been widely assumed that the interaction between the annexins and PC/PS is a purely electrostatic (and hence largely enthalpically driven), here we report that the mechanism of anxa5-lipid binding is mediated by a largely entropy associated process. Similar to other membrane binding proteins (Protein Kinase C) (*43*), we suggest that the release of water and ions from the membrane upon annexin binding is the driving force for anxa5-membrane coupling. Binding analysis of these isotherms shows that anxa5 binds fluid state mixtures with a significantly lower K_d than gel state

mixtures demonstrating that lipid-lipid interactions and protein-protein interactions play a vital role in the binding of anxa5 to the membrane. Analysis of these isotherms show that anxa5 binds fluid state mixtures with a significantly lower K_d than gel state lipids suggesting that as gel state lipids are already ordered, their impetus to binding is reduced compared to binding to fluid state lipids which have more associated waters that can be released. ($K_a=1/K_d$). This result suggests that because gel state lipid tails are already ordered, the affinity of anxa5 for that mixture is reduced. In regard to the binding stoichiometry (n) of these experiments, it is difficult to assess the true meaning of n. Previous binding data regarding the binding of Anx5 to fluid state lipids has reported stoichiometry ranging from 25 to 50 lipids per annexin molecule. Interpretation of the actual number of phospholipids bound per protein molecule is difficult because LUV vesicles were used and not individual lipids or detergents as reported in (*44*) and other studies (*45*) and (*46*). Undoubtedly, the role of trimerization in the membrane binding process increases the effective concentration of lipid that Anx5 can bind because a surface is titrated rather than individual lipids. Interestingly, previous literature reports indicated that Anx5 is not appreciably able to bind to gel state lipids. As (*47*) reported, by use of fluorescence microscopy that monomers do not significantly bind to gel state lipids using fluorescently labeled Anx5 and supported lipid bilayers. In addition, (*48*) reported that binding of gel state lipids (1,2 ditridecanoyl-sn-glycerol-3-phosphocholine (DTPC) and 14:0PS) did not occur using a copelleting assay. Although the heat produced from ITC is weak, this study suggests that anxa5 does indeed bind gel state lipids. The release of water molecules as a significant contributor to binding is consistent with the weaker binding of anxa5 to PC compared to PS as PC has fewer associated water molecules than

PS does (*49*). Such binding is entropically dominated, is also evidenced by the much weaker binding of anxa5 to gel state compared to fluid state lipids (Figures 9 and 10). In that the release of water as an entropic gain is concluded to be the dominant contribution to binding of anxa5 to fluid state lipid, this gain is then offset by the penalty of ordering up of the acyl chains.

With regard to the annexins, evidence exists that binding correlates with enhanced ordering of the acyl chain carbons nearest the headgroup region (*26*); (*50*). Not all biological processes are enthalpically dominated, or, in some cases they require little enthalpy component at all for the interaction. Membrane binding by proteins or peptides can be entropically driven (*43, 51-52*). It is the role of water and ions in this phenomenon that dictates specificity, not enthalpic interactions. Indeed, the hydrophobic effect can dominate to such an event with polypeptide-membrane interactions that the enthalpic contribution can oppose partitioning to the membrane surface by 4 kcal/mol (*53*).

In addition, we also report using ITC data that annexin is unable to bind POPC LUVs in the presence and absence of Ca^{2+}. A recent report (*54*) suggested that Anx5 was able to bind 16:1,18:0 PC (POPC) with high affinity as detected by use of an avidin conjugated Horseradish Peroxidase assay. Our results, using ITC and fluorescence titration methods, were unable to confirm any interaction between anxa5 and POPC vesicles (Data Not Shown). The titration was performed in the presence of high protein concentrations (100μM) and still little heat beyond the heat of dilution was evident.

Table 3: Thermodynamic Parameters of anxa5 Binding to Various Ligands

Sample	Number of Ligand(n)	K_d μM^{-1}	ΔH (kcal/mol)	TΔS (kcal/mol)	ΔG (kcal/mol)
POPC:POPS (15°C)	68 ± 2	13 ± 4.0	-0.274± 0.001	6.2 ± 0.2	-6.5 ± 0.2
DMPC:DMPS (15°C)	53.0 ± 9.0	1700 ± 700	0.117 ± 0.003	3.8 ± 0.3	-3.7 ± 0.3
Ca^{2+} (15°C) (per site)	5.8 ± 0.5	300 ± 20	-2.1 ± 0.1	2.6 ± 0.1	-4.6 ± 0.1

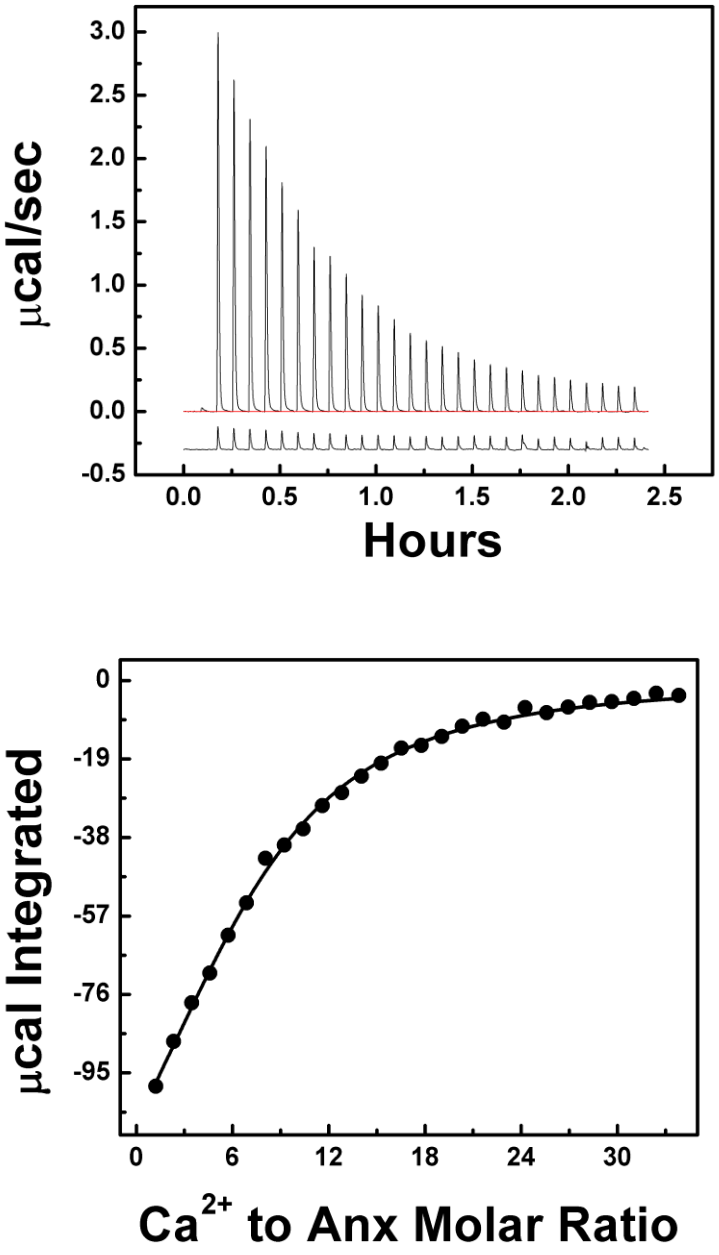

Figure 7 ITC of 10 mM Ca^{2+} injected into 90µM anxa5 in the absence of lipid. Heat of dilution offset below.

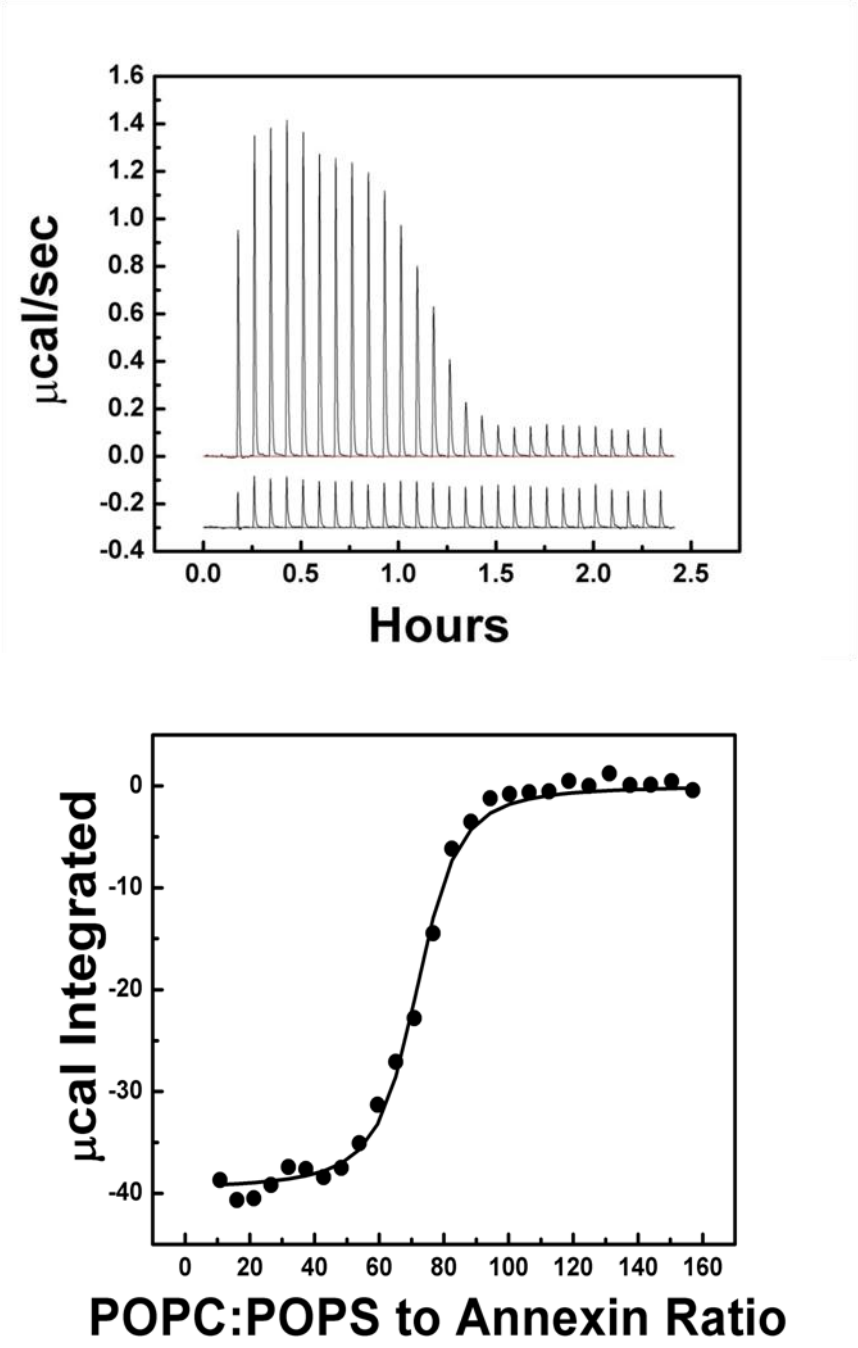

Figure 8 ITC of POPC:POPS (30 mM) Titrated into 20µM anxa5 in the presence of constant 0.5mM Ca^{2+} in 20 mM MOPS,100 mM KCl pH 7.5 at 15°C. Heat of dilution offset below.

Temperature was held at 15°C to compare against gel state lipid titration.

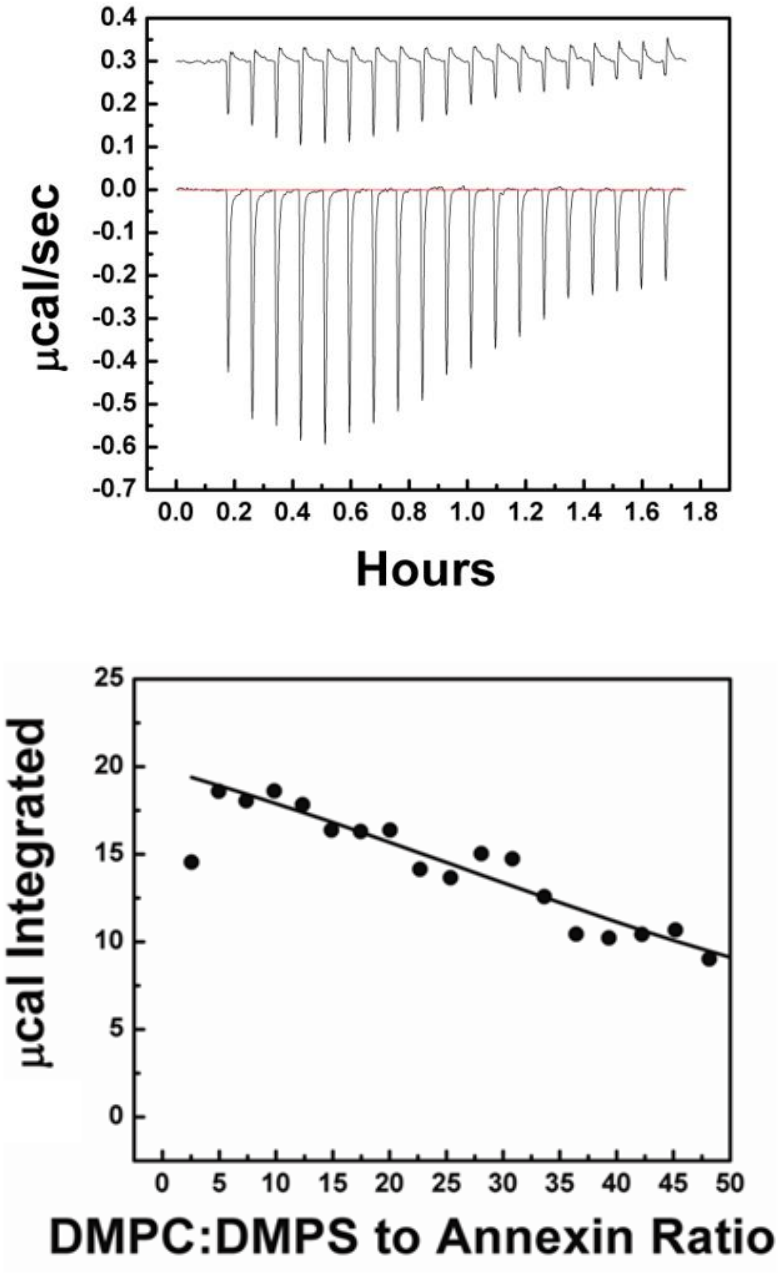

Figure 9 Injection of 30 mM DMPC:DMPS into 100 µM anxa5 in the presence of constant Ca^{2+} (1.0 mM) in 20 mM MOPS,100 mM KCl pH 7.5 at 15°C. Heat of dilution offset above.

High anxa5 concentration used due to weak interaction between anxa5 and gel state lipids. Temperature was held at 15°C to maintain lipids in gel state as lipids will be in transition temperature at 25°C.

CHAPTER 5: ITC CHARACTERIZATION OF A LANTHANIDE BINDING LIGAND

The development of lanthanide binding complexes for *in vivo* use as imaging reagents through fluorescence imaging, (*55-60*) as well as MRI contrast reagents, (*61-65*) has been vital for medical application. Complexes can be injected into a tissue or directed to a specific tissue type that can be used for selective imaging. (*65*) As these complexes will be used *in vivo* it is important that the complexes be both kinetically and thermodynamically stable especially under physiological conditions as free lanthanide ions are toxic (*63, 66*). The ability to sequester lanthanide ions and correspondingly limit the amount of free lanthanide in the blood stream is therefore critical to operation of an effective shift indicator. In our experiments, we utilized ITC to determine the binding of Eu^{3+} to the ligand (Tetra(N-(tert-butyl)-acetamide)-1,13-diamino-3,6,9-trioxadecane) at mimicked physiological conditions. The experiment was performed on a TA Instruments (New Castle, Delaware) Nano ITC at 25°C in the presence of 100mM NaCl at pH 6.0 to simulate physiological conditions. Experiments were also performed attempted at pH 7.5, but the sparing solubility of the ligand was prohibitive for conducting the experiments. In addition, experiments in the presence of 5% ethanol proved to be unusable due to the high heat of dilution of ethanol. The ligand was synthesized as in (*67*) and dried for 24 hours prior to usage. Both the Eu^{3+} titrant and the ligand were dissolved in the same buffer consisting of 10 mM MES (99% Sigma) and 100 mM NaCl (Fluka Trace Select) pH 6.0 that was filtered to remove cation impurities with Bio-Rad 100 chelex resin. The calorimetric sample cell was filled with 1.300 ml of solution consisting of 0.5 mM ligand (Tetra(N-(tert-butyl)-acetamide)-1,13-diamino-3,6,9-trioxadecane),

while the syringe was loaded with 250 μl of 4 mM $Eu(NO_3)_3$. The reference cell was filled with Milli-Q water. The stir speed was 250rpm, and the interval between injections was 300 s. Eu(III) was added in a 1 μl injection to displace air from the syringe followed by 49 x 5 μl injections. The raw heats were integrated, and the heat of dilution was subtracted by injecting 4 mM $Eu(NO_3)_3$ into 10 mM MES, 100 mM NaCl buffer. The subtracted heats were then fit using the independent binding model (single site) from TA Instruments Bindworks software. Other groups have obtained the binding constants of similar ligands by monitoring changes in the UV-Vis absorption spectrum (*68*), (*69*) or with pH potentiometric titrations. (*70*) ITC of Eu(III) and ligand show that the Eu(III) ion binds to the ligand with a binding constant of 9.5 (log K) (Figure 12). For comparison, the binding constants with other lanthanide ligands, such as the popular MRI ligand DOTA and EDTA, are about 23.5 and 17.4 (log K), respectively as determined by potentiometry. (*71*), (*72*) Complexes of tetra amide derivatives of DOTA give lower log K constants of about 13.80. The neutrally-charged amide containing ligands do not have as high binding affinities as comparable ligands containing anionic carboxylic acid groups.

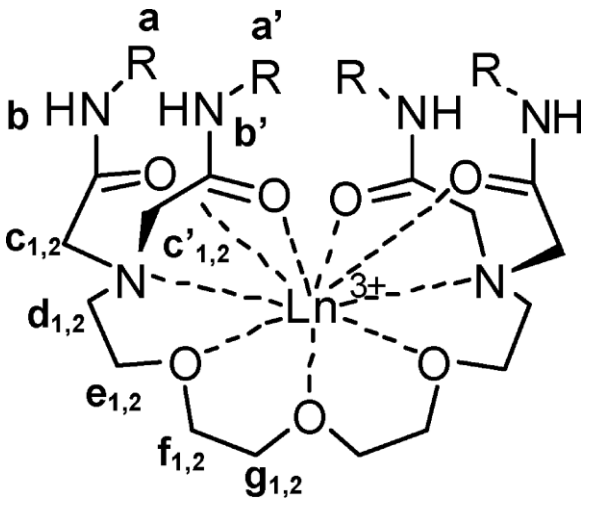

Figure 10 Structure of (Tetra(N-(tert-butyl)-acetamide)-1,13-diamino-3,6,9-trioxadecane)

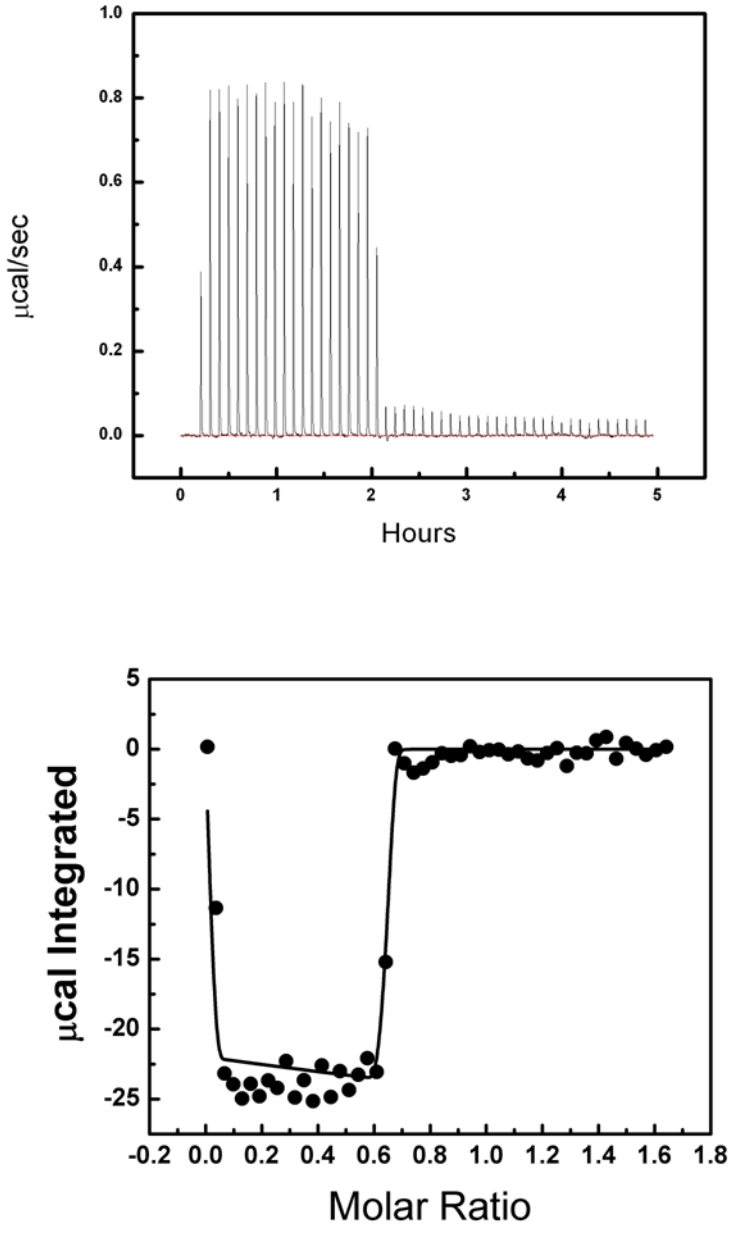

Figure 11 ITC Data for binding of Eu^{3+} to Ligand

CONCLUSIONS

The DSC and ITC results suggest that the consequence of lipid binding by anxa5 is to order the lipids, by a lyotrophic mechanism in which water and ions are released upon anxa5 binding the membrane. This interpretation is based on the increased entropy of the lipid/Ca^{2+} mixture upon addition of anxa5 protein. Utilizing ITC, we find that the enthalpy associated with the binding process for both gel and fluid state lipid mixtures is weak, which is indicative of a similar binding mechanism for the mixtures, albeit that binding of lipid is exothermic for fluid state and endothermic for gel state. In regard to the binding stoichiometry of these experiments, we find that anxa5 binds 50-70 lipid molecules in the presence of Ca^{2+}. Interestingly, previous literature reports indicated that Anx5 is not appreciably able to bind to gel state lipids. Although the heat produced from ITC is weak, this study displays that annexins do indeed bind gel state lipids. Anxa5 displays an entropically dominated binding signature for membrane in both the fluid and gel state. For the fluid state titrations, we report an enthalpy of -0.274± 0.001 kcal/mol and entropy of 6.2 ± 0.2 kcal/mol. For titrations in which gel phase lipids are injected into anxa5 we report an enthalpy of 0.10 ± 0.01 kcal /mol and entropy of 4.3 ± 0.1 kcal/mol, respectively.

We also report that (Tetra(N-(tert-butyl)-acetamide)-1,13-diamino-3,6,9-trioxadecane) has a binding constant of 9.5 (log K), which is significantly lower affinity than MRI reagents currently in therapeutic use.

REFERENCES

1. Singer, S. J., and Nicolson, G. L. (1972) The fluid mosaic model of the structure of cell membranes, *Science 175*, 720-731.
2. Suurkuusk, J., Lentz, B. R., Barenholz, Y., Biltonen, R. L., and Thompson, T. E. (1976) A calorimetric and fluorescent probe study of the gel-liquid crystalline phase transition in small, single-lamellar dipalmitoylphosphatidylcholine vesicles, *Biochemistry 15*, 1393-1401.
3. Gennis, R. B. (1989) *Biomembranes: Molecular Structure and Function*, Springer, New York.
4. Kinnunen, P. K. J. (1991) On the principles of functional ordering in biological membranes, *Chemistry and Physics of Lipids 57*, 375-399.
5. Cevc, G. (1987) How Membrane Chain Melting Properties are Regulated by the Polar Surface of the Lipid Bilayer, *Biochemistry 26*, 6305-6310.
6. Fleming, B. D., and Keough, K. M. W. (1988) Surface respreading after collapse of monolayers containing major lipids of pulmonary surfactant. , *Chemistry and Physics of Lipids 49*, 81-86.
7. Almeida, P. F. F., Vaz, W. L. C., and Thompson, T. E. (1992) Lateral diffusion in the liquid phases of dimyristoylphosphatidylcholine/cholesterol lipid bilayers: a free volume analysis, *Biochemistry 31*, 6739-6747.
8. Crane, J. M., and Tamm, L. K. (2004) Role of cholesterol in the formation and nature of lipid rafts in planar and spherical model membranes, *Biophysical Journal 86*, 2965-2979.
9. Thompson, T. E., and Tillack, T. W. (1985) Organization of glycosphingolipids in bilayers and plasma membranes of mammalian cells, *Annu. Rev. Biophys. Biophys. Chem. 14*, 361-386.
10. Brown, D. A., and Rose, J. K. (1992) Sorting of GPI-anchored proteins to glycolipid-enriched membrane subdomains during transport to the apical cell surface, *Cell 68*, 533-544.
11. Simons, K., and Ikonen, E. (1997) Functional rafts in cell membranes, *Nature 387*, 569-572.
12. Hammond, A. T., Heberle, F. A., Baumgart, T., Holowka, D., Baird, B., and Feigenson, G. W. (2005) Crosslinking a lipid raft component triggers liquid ordered-liquid disordered phase separation in model plasma membranes, *Proc. Natl. Acad. Sci. USA 102*, 6320-6325.
13. Maxfield, F., and Tabas, I. (2005) Role of cholesterol and lipid organization in disease, *Nature 438*, 612-621.
14. Babiychuk, E. B., and Draeger, A. (2000) Annexins in cell membrane dynamics: Ca^{2+}-regulated association of lipid microdomains, *J. Cell Biol. 150*, 1113-1123.
15. Raynal, P., and Pollard, H. B. (1994) Annexins: the problem of assessing the biological role for a gene family of multifunctional calcium- and phospholipid-binding proteins, *Biochim. Biophys. Acta 1197*, 63-93.

16. Rescher, U., and Gerke, V. (2004) Annexins-unique membrane binding proteins with diverse functions, *Journal of Cell Science*.
17. Zobiack, N., Rescher, U., Laarmann, S., Michgehl, S., Schmidt, M. A., and Gerke, V. (2002) Cell-surface attachment of pedestal-forming enteropathogenic E-coli induces a clustering of raft components and a recruitment of annexin 2, *Journal of Cell Science 115*, 91-98.
18. Turnay, J., Lecona, E., Fernández-Lizarbe, S., Guzmán-Aránguez, A., Fernández, M. P., Olmo, N., and Lizarbe, M. A. (2005) Structure-function relationship in annexin A13, the founder member of the vertebrate family of annexins, *Biochem J 389*, 899-911.
19. Gerke, V., and Moss, S. E. (2002) Annexins: From Structure to Function, *Physiological Reviews*.
20. Lu, Y., Bazzi, M. D., and Nelsestuen, G. L. (1995) Kinetics of Annexin-VI, Calicum, and Phospholipid Association and Disssociation, *Biochemistry 34*, 10777-10785.
21. Almeida, P. F. F., Sohma, H., Rasch, K. A., Wieser, C. M., and Hinderliter, A. (2005) Allosterism in membrane binding: a common motif of the annexins?, *Biochemistry 44*, 10905-10913.
22. Zibouche, M., Vincent, M., Illien, F., Gallay, J., and Ayala-Sanmartin, J. (2008) The N-terminal Domain of Annexin 2 Serves as a Secondary Binding Site during Membrane Bridging, *Journal of Biological Chemistry 283*, 22121-22127.
23. Jin, M., Smith, C., Hsieh, H. Y., Gibson, D. F., and Tait, J. F. (2004) Essential role of B-helix calcium binding sites in annexin V-membrane binding, *Journal of Biological Chemistry 279*, 40351-40357.
24. Monod J., W. J., and Changeux J.-P. (1965) On the nature of allosteric transitions: a plausible model., *J. Mol. Biol. 12*, 88-118.
25. Oling, F., Santos, J., Govorukhina, N., Mazeres-Dubut, C., Bergsma-Schutter, W., Oostergetel, G., Keegstra, W., Lambert, O., Lewit-Bentley, A., and Brisson, A. (2000) Structure of membrane-bound annexin A5 trimers: A hybrid Cryo-EM - X-ray crystallography study, *Journal of Molecular Biology 304*, 561-573.
26. Megli, F. M., Selvaggi, M., Liemann, S., and Quagliariello, E. (1998) The calcium-dependent binding of annexin V to phospholipid vesicles influences the bilayer inner fluidity gradient, *Biochemistry 37*, 10540–10546.
27. Wu, F. J., Gericke, A., Flach, C. R., Mealy, T. R., Seaton, B. A., and Mendelsohn, R. (1998) Domain structure and molecular conformation in annexin V/1,2-dimyristoyl-sn-glycero-3-phosphate/Ca2+ aqueous monolayers: A brewster angle microscopy/infrared reflection-absorption spectroscopy study, *Biophysical Journal 74*, 3273-3281.
28. Venien-Bryan, C., Lenne, P. F., Zakri, C., Renault, A., Brisson, A., Legrand, J. F., and Berge, B. (1998) Characterization of the growth of 2D protein crystals on a lipid monolayer by ellipsometry and rigidity measurements coupled to electron microscopy, *Biophysical Journal 74*, 2649-2657.
29. Menke, M., Gerke, V., and Steinem, C. (2005) Phosphatidylserine membrane domain clustering induced by annexin A2/S100A10 heterotetramer, *Biochemistry 44*, 15296-15303.

30. Mo, Y., Campos, B., Mealy, T. R., Commodore, L., Head, J. F., Dedman, J. R., and Seaton, B. A. (2003) Interfacial basic cluster in annexin V couples phospholipid binding and trimer formation on membrane surfaces, *Journal of Biological Chemistry 278*, 2437-2443.
31. Drust, D., and Creutz, C. E. (1988) Aggregation of Chromaffin Granules by Calpactin at micromolar levels of Ca^{2+}, *Nature 331*, 88-91.
32. Elegbede, A. I., Srivastava, D. K., and Hinderliter, A. (2006) Purification of recombinant annexins without the use of phospholipids, *Protein Expression and Purification 50*, 157-162.
33. Brandts, J. F., and Lin, L. N. (1990) Study of strong to ultratight protein interactions using differential scanning calorimetry, *Biochemistry*.
34. Bernhard. (1956) Ionization constants and heats of tris(hydroxymethyl)aminomethane and phosphate buffers., *J Biol Chem 218*, 961-969.
35. Rosengarth, A. (1999) A Comparison of the Energetics of Annexin I and Annexin V, *Journal of Molecular Biology*.
36. Kingsley, P. B., and Feigenson, G. W. (1979) Synthesis of a Perdeuterated Phospholipid - 1,2 Dimyristoyl-sn-Glycero-3- Phosphocholine-D72, *Chemistry and Physics of Lipids 24*, 135-147.
37. Avanti Polar Lipids, I. (2009) *Avanti Polar Lipids Products Catalog*, Fourth ed., Alabaster, AL.
38. Hauser, H., and Shipley, G. G. (1984) Interactions of Divalent- Cations with Phosphatidylserine Bilayer-Membranes, *Biochemistry 23*, 34-41.
39. Freire, E., Mayorga, O. L., and Straume, M. (1990) Isothermal Titration Calorimetry, *Analytical Chemistry 62*, A950-A959.
40. Pace, C. N., Vajdos, F., Fee, L., Grimsley, G., and Gray, T. (1995) How to measure and predict the molar absorption coefficient of a protein, *Protein Science 4*, 2411-2423.
41. Tsien, R. Y. (1980) New Calcium Indicators and Buffers with High Selectivity Against Magnesium and Protons- Design, Synthesis, and Properties of Prototype Structures *Biochemistry 19*, 2396-2404.
42. Wiseman, T., Williston, S., Brandts, J. F., and Lin, L. N. (1989) Rapid measurement of binding constants and heats of binding using a new titration calorimeter, *Analytical Biochemistry 179*, 131-137.
43. Torrecillas, A., Laynez, J., Menendez, M., Corbalan-Garcia, S., and Gomez-Fernandez, J. C. (2004) Calorimetric study of the interaction of the C2 domains of classical protein kinase C isoenzymes with Ca^{2+} and phospholipids, *Biochemistry 43*, 11727-11739.
44. Meers, P., and Mealy, T. (1993) Calcium-Dependent Annexin-V Binding to Phospholipids - Stoichiometry, Specificity, and the Role of Negative Charge, *Biochemistry 32*, 11711-11721.
45. Tait, J. F., Gibson, D., and Fujikawa, K. (1989) Phospholipid binding-properties of Human Placental Anticoagulant Protein-I, A Member of the Lipocortin Family., *Journal of Biological Chemistry 264*, 7944-7949.

46. Jeppesen, B., Smith, C., Gibson, D., and Tait, J. (2008) Entropic and Enthalpic Contributions to Annexin V-Membrane Binding: A COMPREHENSIVE QUANTITATIVE MODEL, *Journal of Biological Chemistry 283*, 6126-6135.
47. Han, J. J., and Boo, D. W. (2009) Reversible Immobilization of Diffusive Membrane-Associated Proteins Using a Liquid-Gel Bilayer Phase Transition: A Case Study of Annexin V Monomers, *Langmuir : The ACS Journal of Surfaces and Colloids*.
48. Patel, D. R., Isas, J. M., Ladokhin, A. S., Jao, C. C., Kim, Y. E., Kirsch, T., Langen, R., and Haigler, H. T. (2005) The conserved core domains of annexins A1, A2, A5, and B12 can be divided into two groups with different Ca^{2+}-dependent membrane-binding properties, *Biochemistry 44*, 2833-2844.
49. Petrache, H. I., Tristram-Nagle, S., Gawrisch, K., Harries, D., Parsegian, V. A., and Nagle, J. F. (2004) Structure and fluctuations of charged phosphatidylserine bilayers in the absence of salt, *Biophysical Journal 86*, 1574-1586.
50. Saurel, O., Cézanne, L., Milon, A., Tocanne, J. F., and Demange, P. (1998) Influence of annexin V on the structure and dynamics of phosphatidylcholine/phosphatidylserine bilayers: a fluorescence and NMR study, *Biochemistry 37*, 1403-1410.
51. Abraham, T., Lewis, R., Hodges, R. S., and McElhaney, R. N. (2005) Isothermal titration calorimetry studies of the binding of a rationally designed analogue of the antimicrobial peptide gramicidin S to phospholipid bilayer membranes, *Biochemistry 44*, 2103-2112.
52. Abraham, T., Lewis, R., Hodges, R. S., and McElhaney, R. N. (2005) Isothermal titration calorimetry studies of the binding of the antimicrobial peptide gramicidin S to phospholipid bilayer membranes, *Biochemistry 44*, 11279-11285.
53. Russell, C. J., Thorgeirsson, T. E., and Shin, Y. K. (1996) Temperature dependence of polypeptide partitioning between water and phospholipid bilayers, *Biochemistry 35*, 9526-9532.
54. Maffey, K. G., Keil, L. B., and DeBari, V. A. (2001) The influence of lipid composition and divalent cations on annexin V binding to phospholipid mixtures, *Annals of Clinical and Laboratory Science 31*, 85-90.
55. Moore, E. G., Samuel, A. P. S., and Raymond, K. N. (2009) From Antenna to Assay: Lessons Learned in Lanthanide Luminescence, *Acc. Chem. Res. 42*, 542-552.
56. Bünzli, J.-C., G. (2006) Benefiting from the unique properties of lanthanide ions, *Acc Chem Res 39*, 53-61.
57. Pedziwiatr, M., Kosareff, N. M., Muller, G., Koposov, A. Y., Nemykin, V. N., Riehl, J. P., and Legendziewicz, J. (2008) Preparation, characterization, and circularly polarized luminescence of lanthanum and europium 1,1'-binaphthyl-2,2'-diyl phosphate complexes, *J. Alloys Compd. 451*, 251-253.
58. Gregolinski, J., Starynowicz, P., Hua, K. T., Lunkley, J. L., Muller, G., and Lisowski, J. (2008) Helical Lanthanide(III) Complexes with Chiral Nonaaza Macrocycle, *J. Am. Chem. Soc. 130*, 17761-17773.

59. Hanaoka, K., Kikuchi, K., Kobayashi, S., and Nagano, T. (2007) Time-Resolved Long-Lived Luminescence Imaging Method Employing Luminescent Lanthanide Probes with a New Microscopy System, *J. Am. Chem. Soc. 129*, 13502-13509.
60. Burroughs, S. E., Eisenman, G., and Horrocks, W. D., Jr. (1992) Characterization of the five-fold calcium binding site of satellite tobacco necrosis virus using europium luminescence spectroscopy: A marked size-selectivity among rare earth ions, *Biophys. Chem. 42*, 249-256.
61. Aime, S., Crich, S. G., Gianolio, E., Giovenzana, G. B., Tei, L., and Terreno, E. (2006) High sensitivity lanthanide(III) based probes for MR-medical imaging, *Coord. Chem. Rev. 250*, 1562-1579.
62. Frey, S. T., Chang, C. A., Carvalho, J. F., Varadarajan, A., Schultze, L. M., Pounds, K. L., and Horrocks, W. D., Jr. (1994) Characterization of lanthanide complexes with a series of amide-based macrocycles, potential MRI contrast agents, using Eu3+ lminescence sectroscopy and mlecular mechanics, *Inorg. Chem. 33*, 2882-2889.
63. Bellin, M.-F. (2006) MR contrast agents, the old and the new, *Eur. J. Radiol. 60*, 314-323.
64. Bottrill, M., Kwok, L., and Long, N. J. (2006) Lanthanides in magnetic resonance imaging, *Chem. Soc. Rev. 35*, 557-571.
65. Misra, S. N., Gagnani, M. A., Devi, I. M., and Shukla, R. S. (2004) Biological and clinical aspects of lanthanide coordination compounds, *Bioinorg. Chem. Appl. 2*, 155-192.
66. Pandya, S., Yu, J., and Parker, D. (2006) Engineering emissive europium and terbium complexes for molecular imaging and sensing, *Dalton. Trans.*, 2757-2766.
67. Dorweiler, J. D., Nemykin, V. N., Ley, A. N., Pike, R. D., and Berry, S. M. (2009) Structural and NMR Characterization of Sm(III), Eu(III), and Yb(III) Complexes of an Amide Based Polydentate Ligand Exhibiting Paramagnetic Chemical Exchange Saturation Transfer Abilities, *Inorganic Chemistry 48*, 9365-9376.
68. Tyeklar, Z., Dunham, S. U., Midelfort, K., Scott, D. M., Sajiki, H., Ong, K., Lauffer, R. B., Caravan, P., and McMurry, T. J. (2007) Structural, kinetic, and thermodynamic characterization of the interconverting isomers of MS-325, a gadolinium(III)-based magnetic resonance angiography contrast agent, *Inorganic Chemistry 46*, 6621-6631.
69. Mundoma, C., and Greenbaum, N. L. (2003) Binding of europium(III) ions to RNA stem loops: Role of the primary hydration sphere in complex formation, *Biopolymers 69*, 100-109.
70. Pasha, A., Tircso, G., Benyo, E. T., Brucher, E., and Sherry, A. D. (2007) Synthesis and characterization of DOTA-(amide)4 derivatives: Equilibrium and kinetic behavior of their lanthanide(III) complexes, *European Journal of Inorganic Chemistry*, 4340-4349.
71. Cacheris, W. P., Nickle, S. K., and Sherry, A. D. (1987) Thermodynamic Study of Lanthanide Complexes of OF 1,4,7-Triazacyclononane-N,N',N''-Triacetic Acid

and 1,4,7,10-Tetraazacyclododecane-N,N',N",N"'-Tetraacetic Acid *Inorganic Chemistry 26*, 958-960.

72. Byegard, J., Skarnemark, G., and Skalberg, M. (1999) The stability of some metal EDTA, DTPA and DOTA complexes: Application as tracers in groundwater studies, *Journal of Radioanalytical and Nuclear Chemistry 241*, 281-290.